Regulation of SREBP during hypoxia requires Ofd1-mediated control of both DNA binding and degradation

Joshua R. Porter[a,*], Chih-Yung S. Lee[b,*,†], Peter J. Espenshade[b], and Pablo A. Iglesias[a]
[a]Department of Electrical and Computer Engineering and [b]Department of Cell Biology, Johns Hopkins University School of Medicine, Baltimore, MD 21205

ABSTRACT **Cells adapt to changes in ambient oxygen by changing their gene expression patterns. In fission yeast, the sterol regulatory element–binding protein Sre1 is proteolytically cleaved under low oxygen, and its N-terminal segment (Sre1N) serves as a hypoxic transcription factor. When oxygen is present, the prolyl hydroxylase Ofd1 down-regulates Sre1N activity in two ways: first, by inhibiting its binding to DNA, and second, by accelerating its degradation. Here we use a mathematical model to assess what each of these two regulatory functions contributes to the hypoxic response of the cell. By disabling individual regulatory functions in the model, which would be difficult in vivo, we found that the Ofd1 function of inhibiting Sre1N binding to DNA is essential for oxygen-dependent Sre1N regulation. The other Ofd1 function of accelerating Sre1N degradation is necessary for the yeast to quickly turn off its hypoxic response when oxygen is restored. In addition, the model predicts that increased Ofd1 production at low oxygen plays an important role in the hypoxic response, and the model indicates that the Ofd1 binding partner Nro1 tunes the response to oxygen. This model quantifies our understanding of a novel oxygen-sensing mechanism that is widely conserved.**

Monitoring Editor
Leah Edelstein-Keshet
University of British Columbia

Received: Jun 13, 2012
Revised: Jul 12, 2012
Accepted: Jul 18, 2012

INTRODUCTION

Nutrient sensing is central to the ability of a cell to maintain homeostasis. Oxygen is an essential nutrient, and the failure of a cell to respond to low oxygen supply (hypoxia) may lead to death of the cell or organism (Semenza, 2010). Hypoxia also plays an important role in the development of diseases such as cancer, heart disease, and stroke (Semenza, 2011). Thus a clear understanding of how cells detect and adapt to hypoxia is needed.

In mammals, the hypoxia-inducible factor (HIF) system is a primary regulator of oxygen homeostasis, sensing oxygen and responding appropriately when oxygen is depleted. HIFα is a transcription factor that, in the absence of oxygen, up-regulates a variety of genes necessary for hypoxic adaptation (Gordan and Simon, 2007). In the presence of oxygen, HIFα is tagged for proteasomal degradation by enzymes in the prolyl hydroxylase domain (PHD) family, which hydroxylate HIFα on two proline residues (Schofield and Ratcliffe, 2005). Moreover, in the presence of oxygen, HIFα is inactivated by the asparaginyl hydroxylase factor inhibiting HIF (FIH), which hydroxylates a particular asparagine residue, preventing HIFα from interacting with its transcriptional coactivator p300 (Hirota and Semenza, 2005). Both the PHDs and FIH are 2-OG-Fe(II)–dependent dioxygenases, which require oxygen as a substrate to perform hydroxylation, providing a natural means of oxygen-dependent HIFα control (Schofield and Ratcliffe, 2005; Ozer and Bruick, 2007).

In fungi, a different mechanism for hypoxic response involves a class of transcription factors known as sterol regulatory element–binding proteins (SREBPs). These proteins are named for their homology to the SREBP proteins in mammals, which function in lipid homeostasis (Osborne and Espenshade, 2009). SREBPs are

This article was published online ahead of print in MBoC in Press (http://www.molbiolcell.org/cgi/doi/10.1091/mbc.E12-06-0451) on July 25, 2012.

*These authors contributed equally to this work.

†Present address: Department of Molecular Biology and Genetics, Johns Hopkins University School of Medicine, Baltimore, MD 21205.

Address correspondence to: Pablo Iglesias (pi@jhu.edu), Peter Espenshade (peter.espenshade@jhmi.edu).

Abbreviations used: ARD, ankyrin repeat domain; FIH, factor inhibiting HIF; HIF, hypoxia-inducible factor; PHD, prolyl hydroxylase domain; SREBP, sterol regulatory element–binding protein.

membrane-bound transcription factors that are activated when liberated from the membrane by proteolytic cleavage. The cleaved N-terminal segment binds to sterol regulatory elements (SREs) in DNA; in fungi this activates a transcriptional program involved in adaptation to hypoxia. This mechanism is broadly conserved, as SREBPs have been found in numerous fungal species (Bien and Espenshade, 2010) and play an oxygen-sensing role necessary for virulence in the pathogenic fungi *Cryptococcus neoformans* (Chang *et al.*, 2007; Chun *et al.*, 2007) and *Aspergillus fumigatus* (Willger *et al.*, 2008; Barker *et al.*, 2012).

One of the best-studied fungal SREBPs is the protein Sre1 in the fission yeast *Schizosaccharomyces pombe* (Hughes *et al.*, 2005). Sre1 is proteolytically cleaved by a mechanism involving components of the ubiquitin-proteasome pathway (Stewart *et al.*, 2011) to form the N-terminal transcription factor Sre1N. Sre1N up-regulates a variety of genes needed for *S. pombe* to survive under hypoxic conditions, including those required for the biosynthesis of ergosterol, heme, sphingolipid, and ubiquinone (Todd *et al.*, 2006). Much like HIFα in mammals, Sre1N is regulated in two ways by an oxygen-sensing system centered on the 2-OG-Fe(II)-dependent dioxygenase Ofd1. First, Ofd1 regulates DNA binding: when oxygen levels are high, Ofd1 binds to Sre1N and blocks Sre1N binding to DNA, inactivating it as a transcription factor (Lee *et al.*, 2011). Second, Ofd1 regulates degradation: when Ofd1 is bound to Sre1N in the presence of oxygen, it accelerates Sre1N degradation (Hughes and Espenshade, 2008). When oxygen levels are low, Ofd1 binds preferentially to the Sre1N competitor Nro1, which keeps it from inhibiting Sre1N binding to DNA or accelerating Sre1N degradation (Lee *et al.*, 2009, 2011). This system is distinct from the HIF system in that Ofd1 performs both the inhibitory function of FIH and the degradative function of the PHDs on the hypoxic transcription factor. Moreover, the enzymatic activity of Ofd1 is not required for either its inhibitory or its degradative function (Hughes and Espenshade, 2008; Lee *et al.*, 2011).

These discoveries, which highlight the novelty of the Sre1 regulatory pathway as an oxygen-sensing system, raise two questions: Are both of these regulatory functions—oxygen-dependent regulation of DNA binding and degradation—necessary for Ofd1 to control Sre1N activity under physiological conditions? If so, what does each function contribute? These are systems-level questions, and answering them experimentally is infeasible, as it would require separating two closely connected functions of a single protein. Because of this, we addressed these questions by a systems-biological approach. In this study, we created a mathematical model of Ofd1 function in the Sre1 pathway consistent with experimental evidence. Because many of the parameters for this model were unknown, we found them by an indirect approach: we performed experiments on yeast in vivo to quantify the behavior of the pathway, then picked parameter sets that yielded behavior in simulation consistent with that observed in vivo. We then conducted experiments in silico, making changes to the model that would be difficult to make in living cells, to determine the roles of Ofd1-regulated DNA binding and degradation of Sre1N.

Our model of the Sre1 pathway in *S. pombe* expands our fundamental understanding of a biochemical system that forms a new paradigm for oxygen sensing in eukaryotes. In addition to yielding insight into properties of the pathway that are difficult to test, the model provides a platform for making testable predictions about the pathway, two of which we discuss here. Because of the broad conservation of the pathway components, our model serves as a building block for deeper investigation of SREBPs and their implications for hypoxic adaptation in a variety of fungal species. Furthermore, Ofd1 has a homologue in human cells called OGFOD1, which has recently been found to play a role in hypoxic cell death (Saito *et al.*, 2010) and the cellular stress response (Wehner *et al.*, 2010). Thus our model may have implications for understanding oxygen sensing in mammals.

RESULTS

Model of oxygen-dependent Sre1N regulation by Ofd1

We created a model of the Sre1 regulatory pathway in *S. pombe* based on its known components and their interactions (Figure 1A). The Sre1 pathway regulates several metabolic pathways, including the ergosterol biosynthetic pathway, to enable their adaptation to hypoxia. Sre1 and Scp1, two endoplasmic reticulum (ER) membrane proteins, form a complex that monitors the level of ergosterol in the ER membrane (Hughes *et al.*, 2005; Porter *et al.*, 2010). When oxygen is low, production of ergosterol is hampered, causing the concentration of ergosterol in cells to decrease as the cells grow. On sensing low ergosterol, the Sre1–Scp1 complex is transported from the ER to the Golgi and cleaved to form the active transcription factor Sre1N, the N-terminal segment of Sre1 (Hughes *et al.*, 2005). Sre1N binds to DNA to up-regulate transcription of numerous genes required for hypoxic adaptation, including those coding for its own precursor, Sre1, many of the Erg enzymes involved in ergosterol production, and Ofd1, a prolyl 4-hydroxylase-like 2-OG-Fe(II) dioxygenase (Hughes *et al.*, 2005; Todd *et al.*, 2006). Ofd1 regulates both the DNA binding and the degradation of Sre1N in an oxygen-dependent manner. In the presence of oxygen, Ofd1 binds to Sre1N and keeps Sre1N from binding to DNA (Lee *et al.*, 2011). Furthermore, in the presence of oxygen, Ofd1 accelerates Sre1N degradation (Hughes and Espenshade, 2008). This degradation requires the E2 ubiquitin-conjugating enzyme Rhp6 and the E3 ubiquitin ligase Ubr1 (Lee *et al.*, 2011). In the absence of oxygen, Ofd1 binds to the competitive inhibitor Nro1, slowing Sre1N degradation and leaving it free to bind to DNA and up-regulate hypoxic gene transcription (Lee *et al.*, 2009, 2011).

On the basis of this evidence, we modeled Ofd1 as having six states: unbound, bound to Nro1, and bound to Sre1N, each oxygenated and nonoxygenated. Because Ofd1 is predicted to be a prolyl hydroxylase (Henri *et al.*, 2010; Kim *et al.*, 2010), we modeled its change in oxygenation simply as oxygen binding. Sre1N thus exists in three states: unbound or "free," bound to nonoxygenated Ofd1, and bound to oxygenated Ofd1. We assumed that free Sre1N is the only form available to bind to DNA and up-regulate gene transcription. We further assumed that the three forms of Sre1N are degraded at different rates.

In wild-type yeast, the Sre1 regulatory pathway has two known ways of sensing oxygen: directly via Ofd1 and indirectly by sensing ergosterol. To study the regulatory function of Ofd1, we used the *sre1N* strain of yeast, in which the *sre1*$^{+}$ gene contains a premature stop codon and produces the N-terminal segment of Sre1 directly without the need for proteolytic cleavage (Figure 1B; Hughes and Espenshade, 2008). This effectively renders the pathway independent of ergosterol, removing a confounding variable. We constructed our mathematical model (Supplemental Materials) based on this modified pathway.

Quantifying the hypoxic response in *sre1N* cells

Determining the unknown parameters in our model required a comprehensive, quantitative data set against which the model could be tested. To generate this data set, we performed three experiments on *sre1N* cells that covered a variety of physiological scenarios. In the steady-state experiment (Figure 2, A–C; see *Materials and*

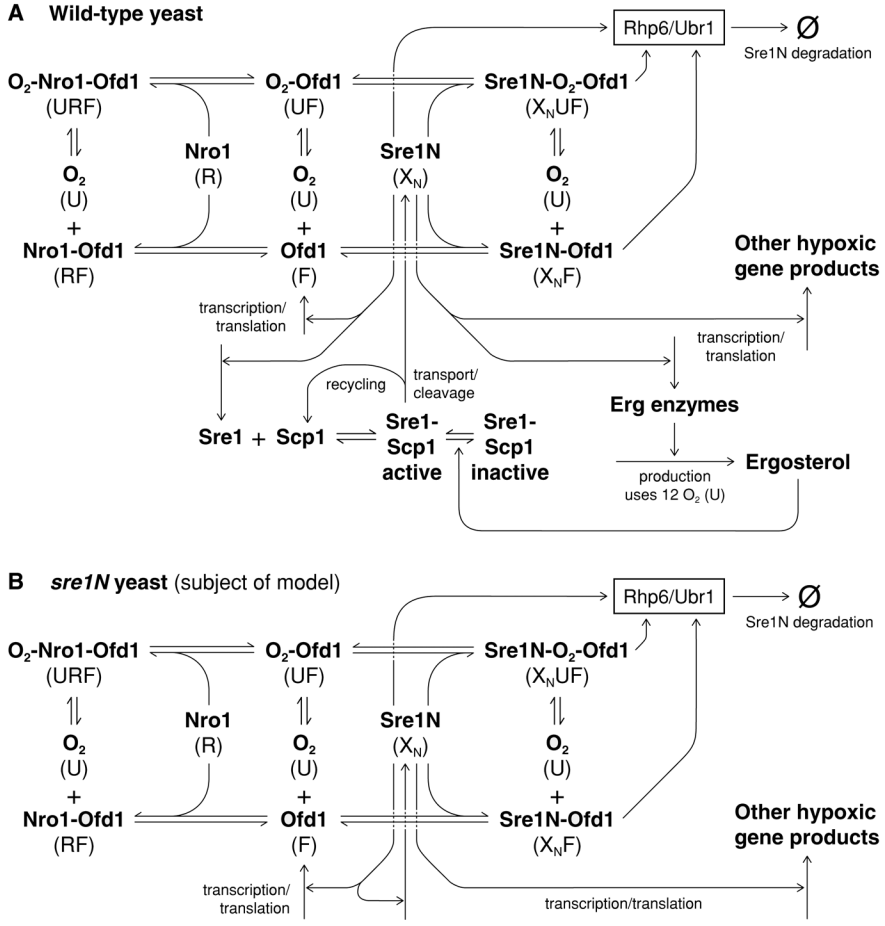

FIGURE 1: The Sre1 regulatory pathway. (A) In wild-type yeast, when the Sre1–Scp1 complex senses low ergosterol, it is transported out of the ER and cleaved to form the active transcription factor Sre1N. Ofd1 regulates the quantity and activity of Sre1N in an oxygen-dependent manner. We modeled Ofd1 as having six states: unbound, bound to Sre1N, or bound to Nro1 at low oxygen or high oxygen. Each state of Ofd1 is degraded with the same rate coefficient (not shown). (B) In *sre1N* yeast, the subject of the model in this article, Sre1N protein is produced directly, bypassing the ergosterol-sensing step. Symbols used in the model equations are in parentheses below each chemical species.

Methods), we grew cells at several levels of oxygen and measured concentrations of *sre1N*$^+$ mRNA, Sre1N protein, and Ofd1 protein in a fixed-size population of cells. Consistent with previous qualitative observations (Hughes and Espenshade, 2008), the steady-state concentration of Sre1N protein remained close to that at atmospheric oxygen for oxygen levels >0.2%. Cells under anoxia showed a ~33-fold increase in Sre1N over cells in atmospheric oxygen (Figure 2B). *sre1N*$^+$ mRNA followed a similar pattern, with consistent mRNA concentrations for oxygen levels >0.5% and a ~12-fold increase in mRNA between normoxia and anoxia (Figure 2A). Ofd1 levels increased ~1.5-fold when cells were shifted from atmospheric oxygen to 1% oxygen; there was no clear further increase at lower levels of oxygen (Figure 2C).

In addition to testing cells at steady state, we performed two experiments to assess the temporal behavior of the pathway. In the hypoxia experiment (Figure 2, D–F), we grew cells at atmospheric oxygen and then shifted them to 0.2% oxygen and measured *sre1N*$^+$ mRNA, Sre1N protein, and Ofd1 protein at time points up to 6 h. Sre1N protein increased slowly at first and faster after ~1 h, reaching a peak ~2–3 h into the experiment and then falling (Figure 2E). *sre1N*$^+$ mRNA followed a similar course (Figure 2D). Ofd1 increased nearly monotonically over the course of the experiment, reaching an approximate plateau after ~2 h (Figure 2F). In the recovery experiment (Figure 2, G and H), we grew cells at 0.2% oxygen for 14 h and then shifted them to atmospheric oxygen and measured *sre1N*$^+$ mRNA and Sre1N protein at time points up to 6 h. Both *sre1N*$^+$ mRNA and Sre1N protein levels fell sharply during the first hour of the experiment, settling to steady levels after ~2 h.

These experiments highlight a modeling caveat: although cells grown in 0.2% oxygen for 6 h had Sre1N concentrations about three times that of cells at normoxic steady state, cells grown in 0.2% oxygen for 14 h had Sre1N concentrations about eight times that of cells at normoxia. We hypothesize that the increase in Sre1N from 6 to 14 h was a result of other long-term hypoxic responses beyond the scope of the pathway considered in our model. Thus our model is most appropriate to understand the short-term response of cells to hypoxia.

Model recreates system behavior with appropriate parameters

Our model of the Sre1 regulatory pathway in *sre1N* cells has 11 fixed parameters (Supplemental Table S1) and 11 unknown parameters (Supplemental Table S2). To find appropriate values for the unknown parameters, we constructed parameter sets by picking seven parameters from appropriate ranges and choosing optimized values for the other four parameters (Supplemental Materials). For each parameter set, we performed seven tests with the model (*Materials and Methods*) to assess whether it could simulate results matching a wide variety of experimental observations. Of more than 10 billion parameter sets tested, 86,011 (<0.001%) passed all seven tests. Figure 3 shows histograms of the parameter values found in these passing parameter sets, including pairwise histograms for two pairs of parameters that showed notable pairwise relationships. (Supplemental Figure S1 shows pairwise histograms for every pair of parameters tested.)

Although no model parameter was determined with perfect precision, most of the parameters were narrowed down to limited ranges, suggesting that the ranges we initially tested were appropriate for characterizing the parameters. For example, k_{dXN}, the rate coefficient for degradation of unbound Sre1N, was between 1.0 and 2.0 h^{-1} in every passing parameter set (Figure 3E). The parameters k_{dXNF}, the rate coefficient for degradation of Sre1N bound to nonoxygenated Ofd1, and K_{XNF}, the dissociation constant between Sre1N and nonoxygenated Ofd1, were found to be pairwise limited (Figure 3A). Among the seven parameters picked initially, K_{UF}, the dissociation constant between Ofd1 and oxygen, and γ, the ratio of Nro1-Ofd1 dissociation constants with/without oxygen, were found to have a tight inverse relationship (Figure 3B).

Figure 2 shows simulations with an example passing parameter set (given in Supplemental Table S2) alongside the experimental

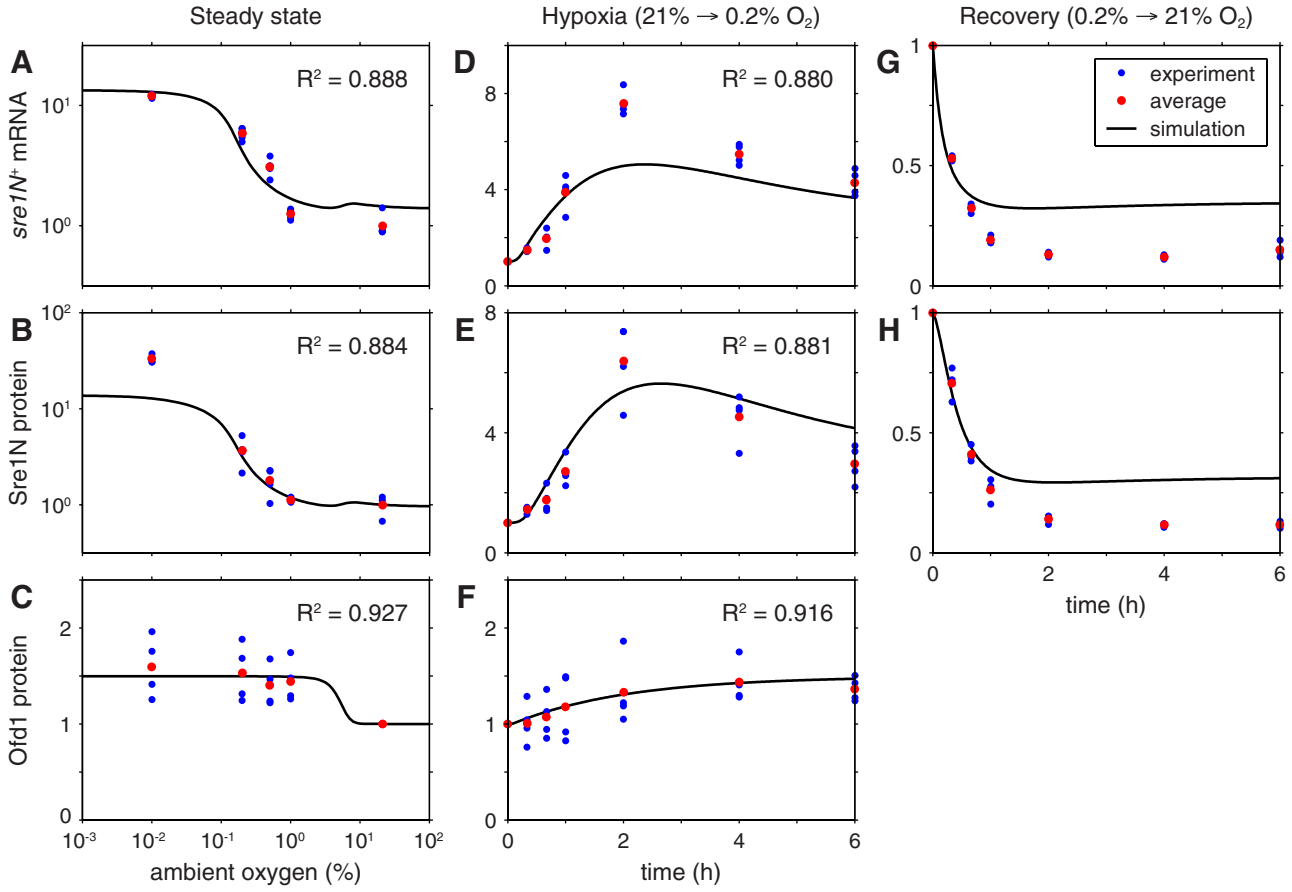

FIGURE 2: Experimental measurements used in model identification. (A–C) *sre1N* cells were grown at different oxygen levels for 12 h (6 h for anoxia, assumed to be 0.01% oxygen). *sre1N*$^+$ mRNA, Sre1N protein, and Ofd1 protein were measured and quantified as described in *Materials and Methods*. All measurements are relative to the average at atmospheric (21%) oxygen. (D–F) *sre1N* cells were grown in atmospheric oxygen and shifted to 0.2% oxygen at $t = 0$. *sre1N*$^+$ mRNA, Sre1N protein, and Ofd1 protein were measured and quantified over 6 h. All measurements are relative to the average at $t = 0$. (G and H) *sre1N* cells were grown at 0.2% oxygen for 14 h and shifted to atmospheric oxygen at $t = 0$. *sre1N*$^+$ mRNA and Sre1N protein were measured and quantified over 6 h. All measurements are relative to the average at $t = 0$. Simulated results in A–H were generated by the model using the example parameter set given in Supplemental Table S2. R^2 values were calculated from logarithms of simulations and data.

data. These simulations fit the data well, showing that the model structure is rich enough to describe the short-term ($t \leq 6$ h) behavior of the system. The simulations captured the order-of-magnitude difference in steady-state *sre1N*$^+$ mRNA and Sre1N protein between high and low oxygen (Figure 2, A and B), the increase and subsequent decrease in *sre1N*$^+$ mRNA and Sre1N protein under hypoxia (Figure 2, D and E), and the increase in Ofd1 protein under low oxygen (Figure 2, C and F). Simulations of the recovery experiment recreated the half-lives of *sre1N*$^+$ mRNA and Sre1N protein (Figure 2, G and H).

Regulation of DNA binding and degradation of Sre1N are both essential functions of Ofd1

With the 86,011 parameter sets that passed the performance requirements, we sought to determine how the two functions of Ofd1—regulation of DNA binding and degradation of Sre1N—contribute to the performance of the system. In one set of tests, we disabled Ofd1-regulated DNA binding in silico by modifying the model so that all Sre1N, not just free Sre1N, could up-regulate *sre1N*$^+$ transcription. This corresponds to replacing the $[X_N]$ terms in Supplemental Eq. S1 with $[X_{NT}]$ terms. In another set of tests, we disabled Ofd1-regulated degradation by modifying the model so that Sre1N bound to Ofd1 was degraded with the same rate coefficient as unbound Sre1N. This corresponds to replacing the parameters k_{dXNF} and k_{dXNUF} with k_{dXN} in Supplemental Eq. S2. We note that both of these modifications would be difficult if not impossible to make in vivo because both effects are the consequence of Ofd1 binding to Sre1N.

In each set of tests, for each parameter set, we quantified steady-state model performance by the regulation ratio—the ratio of total Sre1N at steady state under anoxia (0.01% oxygen) to that under normoxia (21% oxygen). We quantified dynamic model performance by the Sre1N doubling time (time for Sre1N to reach twice its initial concentration) in cells shifted from normoxia to hypoxia (0.2% oxygen) and by the Sre1N half-life (time for Sre1N to fall to half its initial concentration) in cells shifted from hypoxia to normoxia. Figure 4 shows histograms of these three performance metrics and how they changed when regulated DNA binding (Figure 4, A, C, and E) or degradation (Figure 4, B, D, and F) was removed from the model.

Disabling regulated DNA binding in the model had a clear, universal negative effect on performance. For every parameter combination tested, this change decreased the regulation ratio to <3.0,

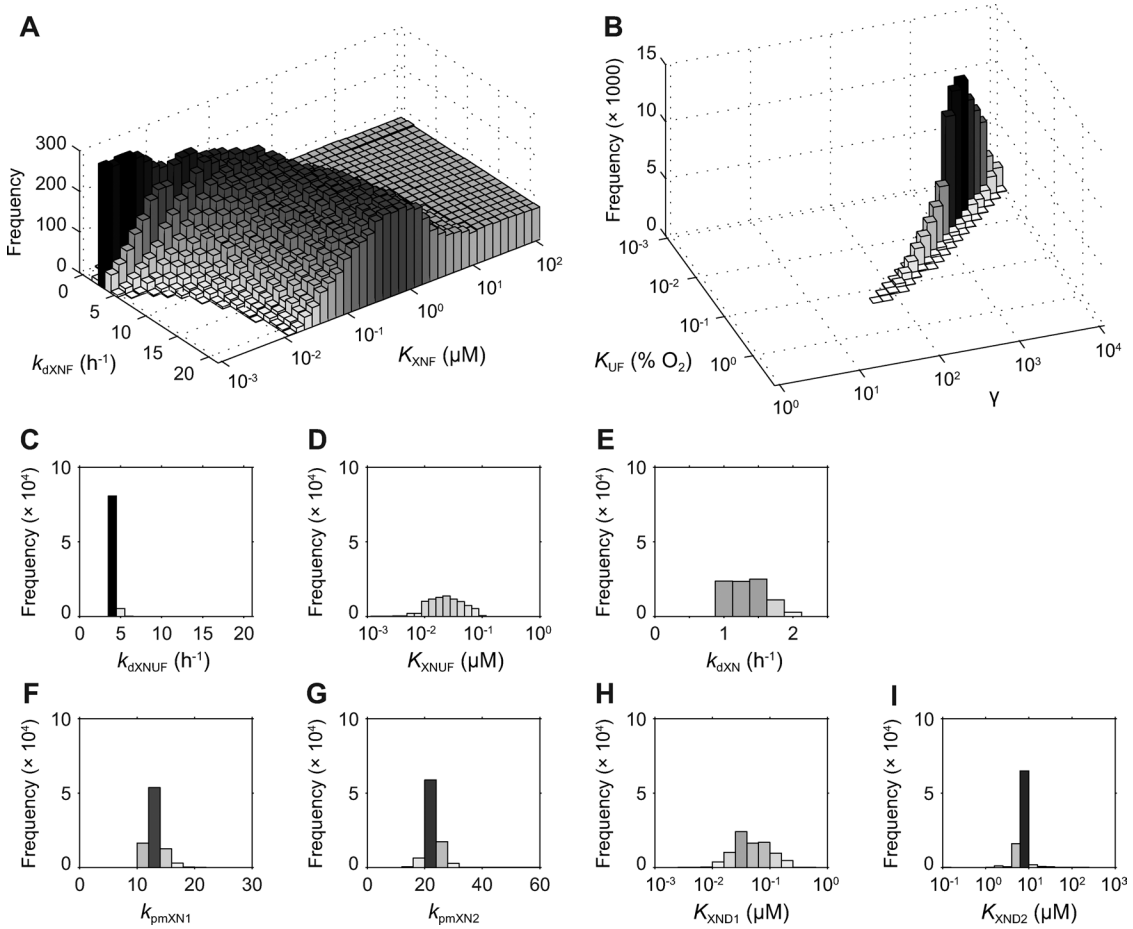

FIGURE 3: Histograms of model parameters found in the parameter sets that passed all seven tests. "Frequency" refers to the number of times each value of each parameter appeared in these passing parameter sets. (A) k_{dXNF} is the rate coefficient for degradation of Sre1N bound to nonoxygenated Ofd1; K_{XNF} is the dissociation constant between Sre1N and nonoxygenated Ofd1. (B) K_{UF} is the dissociation constant between Ofd1 and oxygen; γ is the ratio of dissociation constants between Nro1 and Ofd1 with/without oxygen. (C) k_{dXNUF} is the rate coefficient for degradation of Sre1N bound to oxygenated Ofd1. (D) K_{XNUF} is the dissociation constant between Sre1N and oxygenated Ofd1. (E) k_{dXN} is the rate coefficient for degradation of unbound Sre1N. (F) k_{pmXN1} is the transcription rate of *sre1N*$^+$ when a single Sre1N molecule is bound to its promoter. (G) k_{pmXN2} is the transcription rate of *sre1N*$^+$ when two Sre1N molecules are bound to its promoter. (H) K_{XND1} is the dissociation constant between Sre1N and the first *sre1N*$^+$ binding site. (I) K_{XND2} is the dissociation constant between Sre1N and the second *sre1N*$^+$ binding site (i.e., with a molecule already bound to the other site). A full set of pairwise parameter histograms is shown in Supplemental Figure S1. Bars are shaded according to their height.

compared with 10–26 in control simulations (Figure 4A). The loss of Sre1N regulation was so great that Sre1N never doubled in the hypoxia simulations (Figure 4C) and never halved in the recovery simulations (Figure 4E). Disabling regulated degradation had a similar negative effect on performance, although the effect was weak for some parameter sets. With this change, the regulation ratio decreased to a maximum of 8.1; it was <3.0 for 73% of parameter sets (Figure 4B). Similarly, the Sre1N doubling time under hypoxia increased at least 5.8% in every case; it increased at least 50% for 84% of parameter combinations tested (Figure 4D). One effect was strong and clear, however: without regulated degradation, the Sre1N half-life during recovery increased at least 73% in every case tested (Figure 4F).

From these results, we conclude that regulating the DNA binding of Sre1N is an essential function of Ofd1; the Sre1 regulatory system is virtually nonfunctional without it. We further conclude that regulated Sre1N degradation is required for the system to quickly shut down its hypoxic response when it is no longer needed. Regulated degradation may increase the extent of Sre1N regulation and speed up the hypoxic response as well, but determining this for sure would require further experimentation to narrow the set of parameter combinations. It is safe to say, however, that regulated degradation contributes to the robustness of the pathway, as removing it shrinks the space of parameters yielding the observed level of performance.

A graphical explanation for the effects of the Ofd1 regulatory functions

Our model provides a way to understand intuitively how removing the regulatory functions of Ofd1 affects the ability of the Sre1 pathway to sense oxygen. For the example parameter set given in Supplemental Table S2, Figure 5A shows the rates of Sre1N production (red) and degradation (blue) in the model as a function of oxygen and Sre1N levels, with *sre1N*$^+$ mRNA and Ofd1 protein levels taken

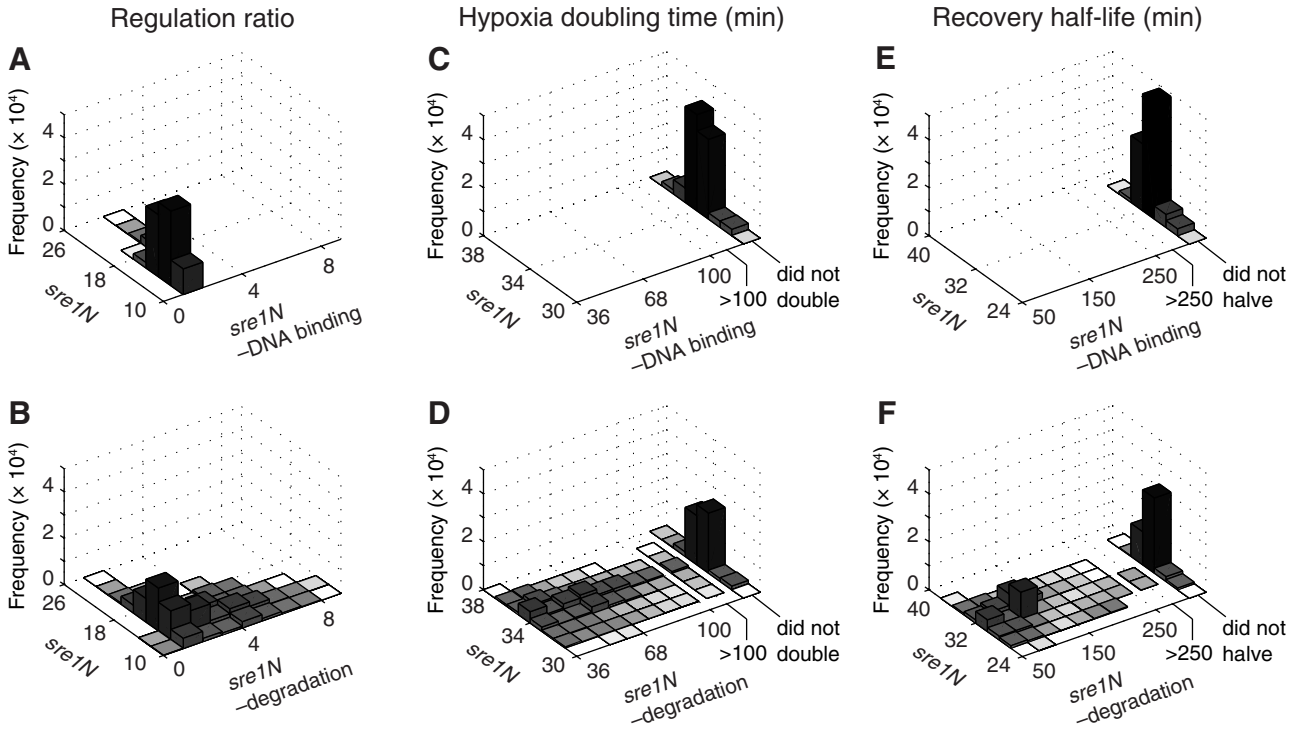

FIGURE 4: Histograms of performance metrics in the model show the effects of disabling the regulatory functions of Ofd1. Histograms show the number of parameter sets (out of those passing all seven tests) that attained the specified performance metrics in two models. (A, C, E) Comparison of the *sre1N* model with the same model lacking regulated DNA binding of Sre1N. (B, D, F) Comparison of the *sre1N* model with the same model lacking regulated degradation of Sre1N. (A, B) Comparison of the regulation ratio—the ratio of Sre1N protein at steady state under anoxia (0.01% oxygen) to that under normoxia (21% oxygen). (C, D) Comparison of the doubling time (time to twice initial concentration) of Sre1N in cells subjected to hypoxia (0.2% oxygen). (E, F) Comparison of the half-life (time to half initial concentration) of Sre1N in cells grown to steady state in hypoxic conditions and returned to normoxia at $t = 0$. Bars are shaded according to the logarithm of their height.

to be at steady state. Sre1N reaches its steady state when it is produced and degraded at the same rate, that is, where the red surface meets the blue surface. When oxygen is high, Ofd1 reduces the amount of Sre1N available to bind to DNA and up-regulate its own production, bending the red (production) surface downward. At the same time, Ofd1 causes Sre1N to degrade faster at high oxygen, which bends the blue (degradation) surface upward. The combined effect is that the surfaces intersect, that is, the steady state occurs, at a 12.8-fold higher level of total Sre1N when oxygen is low than when oxygen is high (Figure 5B).

Disabling Ofd1-regulated DNA binding (Figure 5C) changes the Sre1N production rate so that it depends only on Sre1N and not on oxygen. Consequently, the red (production) surface no longer bends downward at high oxygen levels. With the blue (degradation) surface the same as in the standard model, the two surfaces intersect at a much higher level of Sre1N when oxygen is high, removing nearly all of the oxygen-dependent Sre1N regulation (Figure 5D). Disabling Ofd1-regulated degradation (Figure 5E) lowers the slope of the blue (degradation) surface (since degradation happens at a lower rate) and flattens it (since degradation no longer depends on changing Ofd1 levels). With the red (production) surface the same as in the standard model, the two surfaces intersect in a much different way (Figure 5F) such that the oxygen-dependent Sre1N regulation completely disappears. As noted earlier, this effect does not occur for every passing parameter set; one can imagine from Figure 5E that a small change in parameters, particularly the rate coefficient for degradation of unbound Sre1N, could shift the surfaces to produce a greater degree of regulation.

Increased Ofd1 production explains Sre1N overshoot during hypoxia

The rise and subsequent fall ("overshoot") of both *sre1N*$^+$ mRNA and Sre1N protein during hypoxia (Figure 2, D and E) was an unexpected experimental finding. Such an overshoot indicates that the oxygen sensor in the Sre1 pathway contains a negative feedback loop, a mechanism that acts to oppose a change in the output (Sre1N) caused by a change in the input (oxygen). Although Sre1N overshoot during hypoxia has been observed in wild-type cells (Hughes *et al.*, 2005, 2007), it was believed to be a consequence of the negative feedback on Sre1N production due to increased ergosterol synthesis and inhibition of Sre1 cleavage. Because the machinery for sensing ergosterol is bypassed in the *sre1N* cells used in our experiments, the Sre1 pathway must contain at least one additional source of negative feedback to produce the observed effect.

We hypothesized that the Sre1N overshoot during hypoxia could be explained by increased Ofd1 production under low oxygen, as Ofd1 is a negative regulator of Sre1N quantity and activity. *ofd1*$^+$ is a known target gene of Sre1N (Todd *et al.*, 2006), and we had modeled the rate of Ofd1 production as a simple function of oxygen (Supplemental Eq. S12). To test our hypothesis using the model, we set the rate of Ofd1 production at low oxygen (k_{pF}^{lowU}) equal to that at high oxygen (k_{pF}^{highU}) and simulated cells shifted to hypoxia for 12 h.

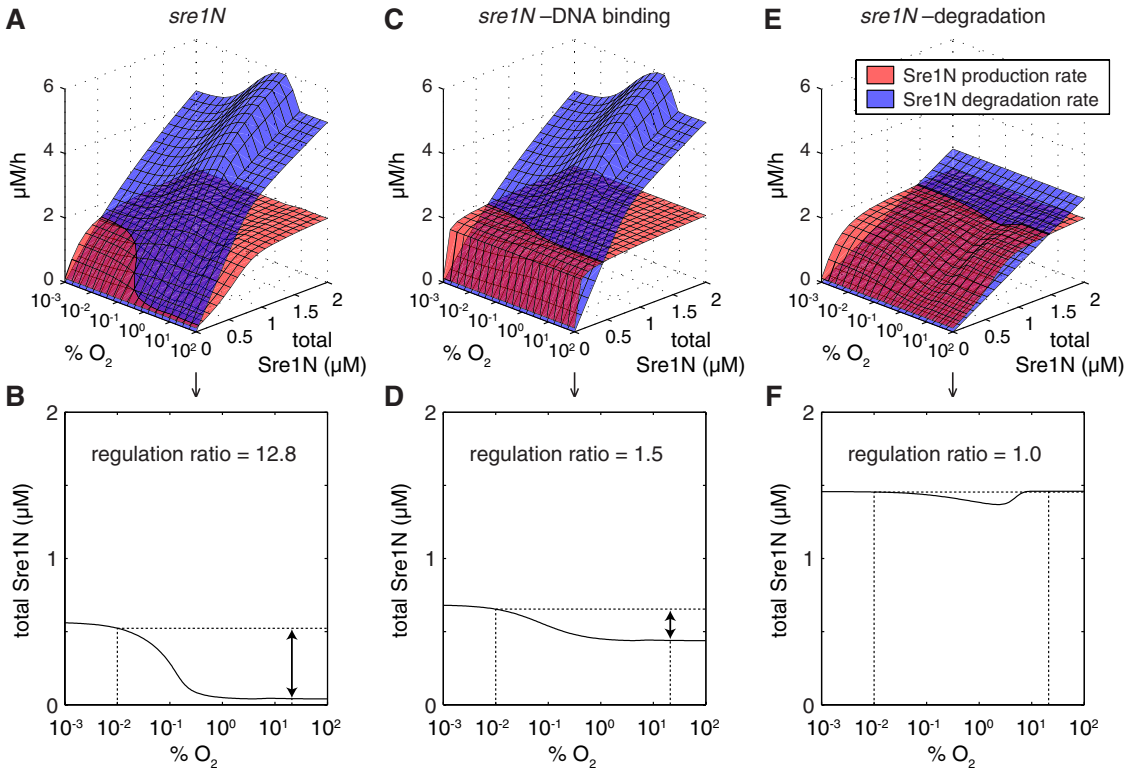

FIGURE 5: Model analysis shows the contribution of the two regulatory functions of Ofd1 to Sre1N regulation. (A, B) With the example parameter set given in Supplemental Table S2, we computed the rate of Sre1N production (red surface) and degradation (blue surface) in the model as a function of oxygen and Sre1N levels. *sre1N*$^+$ mRNA and Ofd1 protein levels are taken to be at steady state. (C, D) We repeated this for the model without regulated DNA binding. This changes the Sre1N production rate but not the degradation rate. (E, F) We also repeated this for the model without regulated degradation. In this case the Sre1N production rates are the same as in the unmodified model, but the degradation rates are different. (B, D, F) Bottom, the projection of the steady-state curve—the points at which Sre1N production and degradation rates are equal—onto the oxygen-Sre1N plane. The regulation ratio is the ratio of total Sre1N under anoxia (0.01% oxygen) to that under normoxia (21% oxygen).

For each of the 86,011 model parameter sets that met the performance requirements, the overshoot of Sre1N (and *sre1N*$^+$ mRNA) completely disappeared when increased Ofd1 production under low oxygen was removed from the model. Figure 6 shows an example of this effect from model simulations with the example parameter set given in Supplemental Table S2. Thus the model predicts that increased Ofd1 production under low oxygen could cause the overshoot in Sre1N observed in *sre1N* cells subjected to hypoxia.

Tuning the oxygen sensitivity of the system with Nro1

In the HIF system, ankyrin repeat domain (ARD) proteins compete with HIFα for access to FIH in an oxygen-dependent manner (Cockman *et al.*, 2009). In the Sre1 regulatory pathway, Nro1 functions similarly, competing with Sre1N for access to Ofd1. This interaction is critical to the function of the system, as *sre1N* cells lacking Nro1 do not have increased Sre1N levels when subjected to hypoxia (Lee *et al.*, 2009). In the HIF system, a predicted role of the ARD proteins is to shape the response of HIFα, fine tuning it with respect to oxygen (Cockman *et al.*, 2009; Schmierer *et al.*, 2010). Although we assumed a constant concentration of Nro1 in our model, we sought to determine to what extent changes in Nro1 levels could play a similar role in shaping the behavior of the Sre1 pathway.

Using the model, we tested the effect of doubling or halving the Nro1 concentration on the hypoxic response of the Sre1 pathway (Figure 7). We simulated levels of *sre1N*$^+$ mRNA and Sre1N protein at steady state, under hypoxic treatment, and under recovery from hypoxia for all 86,011 passing model parameter sets. Of note,

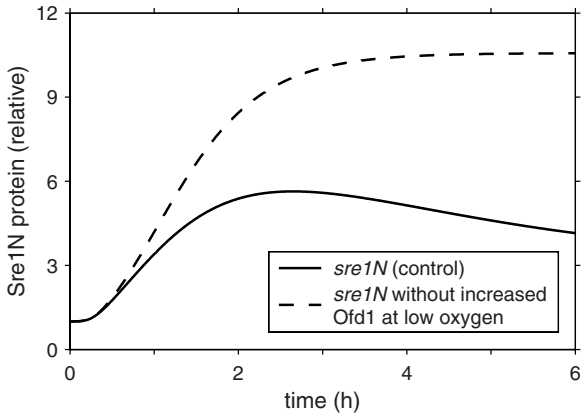

FIGURE 6: Increased Ofd1 production under low oxygen creates the Sre1N overshoot during hypoxia in *sre1N* cells. In both simulations shown, cells at normoxic steady state were shifted to hypoxia (0.2% oxygen) at $t = 0$. Sre1N levels are relative to that at $t = 0$. The example parameter set given in Supplemental Table S2 was used for these simulations.

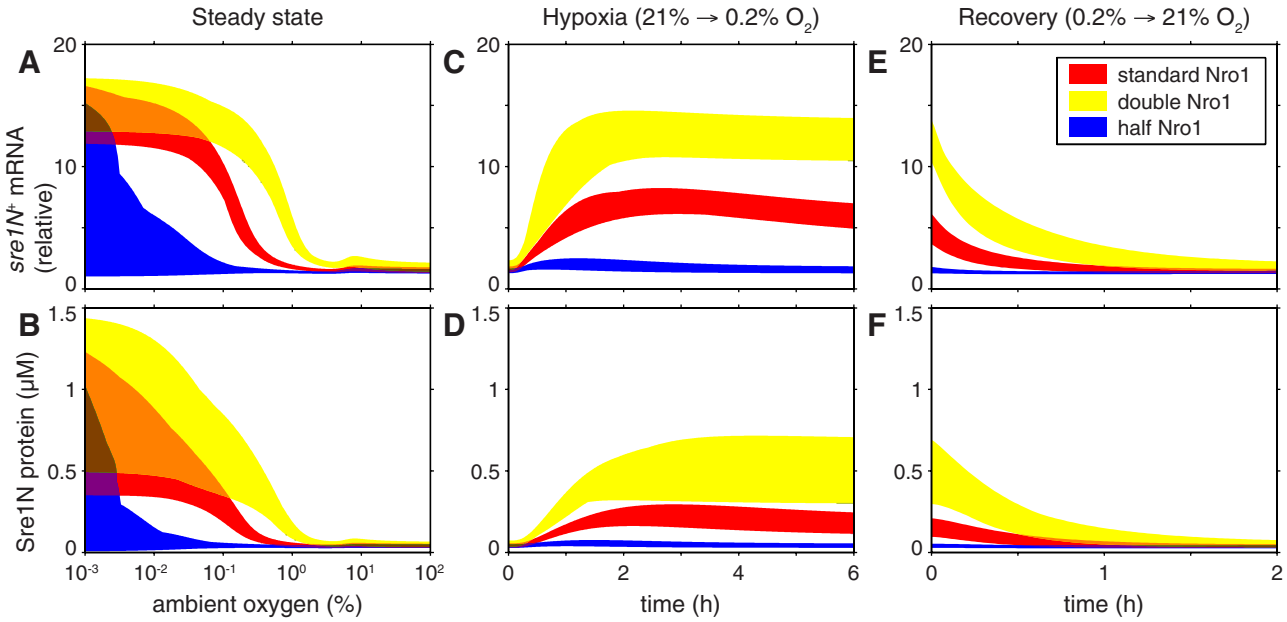

FIGURE 7: Changing the concentration of Nro1 in the model tunes the hypoxic response with respect to oxygen. For each of the 86,011 model parameter sets that met the performance requirements, we computed the steady-state levels (A, B), trajectories during hypoxia (C, D), and trajectories during recovery from hypoxia (E, F) of *sre1N*$^+$ mRNA and Sre1N protein as in Figure 2. The shaded regions for standard Nro1 ($[R_T] = 1.4$ μM), double Nro1 ($[R_T] = 2.8$ μM), and half Nro1 ($[R_T] = 0.7$ μM) contain the response generated by each parameter set.

doubling the Nro1 concentration consistently shifted the threshold for Sre1N up-regulation at steady state to a higher level of oxygen (Figure 7, A and B). Consequently, Sre1N rose to a higher level in the hypoxia simulation (Figure 7, C and D) and fell from a higher level in the recovery simulation (Figure 7, E and F). Conversely, halving the Nro1 concentration consistently shifted the threshold for Sre1N up-regulation at steady state to a lower level of oxygen (Figure 7, A and B), leading to weak hypoxic responses in time (Figure 7, C and F). Thus the model predicts that changing the Nro1 concentration is a plausible way of tuning the Sre1 pathway to activate the hypoxic response at different levels of oxygen.

DISCUSSION

One goal of systems biology is to expose what is obscure in the obvious, that is, what unexpected properties emerge when biological parts are combined to form systems. In this study, we constructed a model of the oxygen sensor in the Sre1 regulatory pathway to investigate how its components work together to create a hypoxic response. We framed the model structure according to our prior knowledge and then selected parameters that yielded simulated results consistent with a variety of experimental observations. The model structure was rich enough to make this possible, suggesting that our knowledge of the system covers the essential interactions that drive the hypoxic response. We then used the model to investigate two ways that the prolyl hydroxylase Ofd1 regulates the transcription factor Sre1N in an oxygen-dependent manner. Although these two regulatory functions are not easily separable in vivo, we removed them from the model individually to determine what each contributes to the overall performance of the system. We found that the Ofd1 function of blocking Sre1N binding to DNA is essential to achieve oxygen-dependent Sre1N regulation. The second Ofd1 function of accelerating Sre1N degradation is essential for the pathway to recover quickly, as observed when oxygen is restored after a period of hypoxia.

Ofd1 represents a novel paradigm for an oxygen sensor in that a single protein regulates both inhibition and degradation of a hypoxic transcription factor. In contrast, these functions are performed independently by two enzymes in the HIF system, the other major paradigm for oxygen sensing in eukaryotes. The dual mechanisms of action of Ofd1 are described by our six-state model, in which Ofd1 can be unbound, bound to Nro1, or bound to Sre1N, oxygenated or nonoxygenated. This amounts to a competitive setup in which Sre1N competes with Nro1 to bind to Ofd1; the relative affinity of Ofd1 for the two is modulated by oxygen. This regulation-through-variable-competition motif is also found in the HIF system, in which HIFα competes with ARD proteins for access to FIH, and the terms of this competition depend on available oxygen (Cockman *et al.*, 2009). The HIF system involves enzymes (FIH, PHDs) modifying substrates (HIFα, ARD proteins) and has been modeled as such (Kohn *et al.*, 2004; Qutub and Popel, 2006, 2007; Dayan *et al.*, 2009; Schmierer *et al.*, 2010). In contrast, Ofd1 is known to bind both Sre1N and Nro1 (Lee *et al.*, 2009, 2011) but is not known to enzymatically modify either, and Ofd1 enzyme activity is not required for it to inhibit DNA binding or accelerate degradation of Sre1N (Hughes and Espenshade, 2008; Lee *et al.*, 2011). Accordingly, our model describes the binding and unbinding of Ofd1 without assuming enzymatic activity, and this is sufficient to replicate the observed behavior of the Sre1 pathway (Figure 2). Thus Ofd1 serves as the central point of a simpler version of the HIF system.

By combining the six-state model of Ofd1 with models of Sre1N-dependent *sre1N*$^+$ transcription and oxygen-dependent *ofd1*$^+$ transcription, our model shows how a complex system of biological control logic responds to low oxygen by producing an order-of-magnitude increase in a hypoxic transcription factor. This system can be considered a feedforward mechanism with respect to the metabolic pathways it regulates, as it senses an environmental disturbance that would alter the function of those pathways (low oxygen) and acts preemptively to compensate. Embedded in this

feedforward mechanism is the positive feedback of Sre1N on its own production, which has been shown to be necessary for strong Sre1N up-regulation (Hughes *et al.*, 2009). Moreover, although we approximated Ofd1 production in the model as a function of oxygen, *ofd1*$^+$ is a known target gene of Sre1N (Todd *et al.*, 2006), and thus the increased production of Ofd1 at low oxygen can be considered a negative feedback path within the larger feedforward mechanism. Our model predicts that in *sre1N* cells subjected to hypoxia, this negative feedback path is responsible for the fall in Sre1N after its increase (Figure 6). We conjecture that this Sre1N overshoot allows a faster response to hypoxia in the same way that overshoots in man-made control systems allow faster responses to changing inputs. The effect of this negative feedback path is unknown in wild-type cells, which combine the control logic described here with the additional negative feedback of ergosterol repressing Sre1 transport and cleavage (Porter *et al.*, 2010). However, on the basis of our results here, we surmise that this hidden negative feedback path may play a previously unappreciated role in the wild-type hypoxic response, suggesting a course for further experimentation.

In addition to this testable prediction about the effect of Ofd1 production, our model makes the prediction that the oxygen threshold for increasing Sre1N can be tuned by adjusting levels of Nro1 (Figure 7). This is yet another resemblance to the HIF system, in which ARD proteins are predicted to play a similar role in tuning the oxygen threshold for HIFα up-regulation (Cockman *et al.*, 2009; Schmierer *et al.*, 2010). Although we assumed a constant concentration of Nro1 for modeling purposes, this mechanism could be a means by which other processes in the cell influence the Sre1 pathway through changing Nro1 levels or activity. Furthermore, this mechanism could facilitate evolutionary adaptation, providing a way of retuning the system in response to selective pressure without fundamentally changing its structure. Validating the predicted effect experimentally and looking deeper into the physiological role of Nro1 are interesting matters for future investigation.

In developing the model presented here, we used an exhaustive parameter search method, which constrained the space of plausible model parameters by identifying those consistent with a variety of observations about the function of Ofd1 in the Sre1 pathway (*Materials and Methods*). This method, while computationally intensive, has several important features that made it appropriate for identifying the parameters of this model. First, it thoroughly explores the parameter space, unlike optimization-based parameter search methods, which can get "stuck" in one region of the parameter space and miss better solutions in other regions. To be thorough, the exhaustive method requires a sufficiently fine grid for sampling the parameter space. Second, the exhaustive method circumvents problems with model identifiability by providing an entire set of solutions consistent with observations. For this model, the difficulty of obtaining reliable measurements at very low oxygen levels created an identifiability problem that affected the parameters K_{XNF} and k_{dXNF}, which govern Sre1N–Ofd1 binding and degradation in the absence of oxygen. Although these parameters were poorly constrained (Figure 3A), we were still able to draw conclusions from the model by examining what was uniformly true for all consistent parameter sets. Third, the exhaustive method can easily incorporate data from other models that have a known relationship to the model being identified. In this case, we incorporated data from several strains of yeast undergoing several types of treatment into the model identification process (*Materials and Methods*).

Although the model presented here describes the *sre1N* strain of *S. pombe*, it is directly applicable to understanding wild-type yeast, as the *sre1N* mutation simply bypasses the machinery for ergosterol-dependent Sre1 cleavage in *S. pombe*. Less directly, this model may be applicable to understanding SREBP pathways in other species of fungi, many of which are natural permutations of that in *S. pombe* (Bien and Espenshade, 2010). One known limitation of the model is that it does not accurately describe the cellular responses to long-term hypoxia or highly anoxic conditions (Figure 2); one can imagine that such extreme stimuli would generate responses well beyond that of Ofd1. Nevertheless, the model is still relevant under such conditions to describe the Ofd1-generated component of the hypoxic response.

Overall, the model presented here advances our understanding of the Ofd1 oxygen sensor in the *S. pombe* SREBP pathway from qualitative to quantitative. Physiologically, this sensor functions in tandem with an ergosterol sensor (Porter *et al.*, 2010) to control ergosterol production along with other processes affected by hypoxia. Present studies focus on modeling this multiple-input, multiple-output control system to better understand regulation in this larger network. Ultimately, this model may be useful for understanding OGFOD1, the orthologue of Ofd1 in mammalian cells, which is involved in hypoxic signaling for cell death (Saito *et al.*, 2010) and stress responses (Wehner *et al.*, 2010). It remains to be seen whether OGFOD1 mediates a general hypoxic response in the manner of Ofd1, but our model provides a starting point for understanding quantitatively how such a response would work.

MATERIALS AND METHODS

Yeast strains and culture

Yeast cell culture and immunoblot analysis were performed as described previously (Hughes *et al.*, 2005). Haploid *S. pombe* strains for hypoxic experiments were grown to exponential phase at 30°C in rich medium containing yeast extract plus supplements (YES; 225 μg/ml each of histidine, leucine, adenine, lysine, and uracil; Hughes *et al.*, 2005). Yeast strains containing plasmids were grown overnight in Edinburgh minimal medium and switched to rich medium for an additional 6 h before cells were harvested. Protein and RNA extraction were performed as previously described (Hughes *et al.*, 2005). Hypoxic and anoxic growth conditions were maintained using an In Vivo 400 hypoxia workstation (Biotrace, Cincinnati, OH) as described previously (Hughes *et al.*, 2005; Todd *et al.*, 2006). The yeast strains used in this work (Supplemental Table S3) were derived from wild-type *S. pombe* by standard genetic techniques (Bähler *et al.*, 1998).

Plasmids

pAH2 and *pAH5* encode truncated N-terminal fragments of Sre1 (amino acids 1–440) under control of the constitutive cauliflower mosaic virus promoter. These plasmids were constructed by inserting the appropriate PCR fragment of *sre1*$^+$ cDNA into the *Bam*HI/*Sal*I sites of pSLF101 (Forsburg, 1993).

Antibodies

Polyclonal antiserum and affinity-purified immunoglobulin G recognizing Sre1 (amino acids 1–260), Nro1, and Ofd1 were generated as described previously (Hughes *et al.*, 2005; Lee *et al.*, 2009). Anti-Myc (9E10) antibody was obtained from Santa Cruz Biotechnology (Santa Cruz, CA).

Determination of Sre1N expression level under different oxygen concentrations

For steady-state experiments, *sre1N* cells were grown in rich medium to a density of 1×10^7 cells/ml and then transferred into the hypoxia workstation at different oxygen concentrations (1, 0.5, or

0.2%, anoxia). After growing for 12 h under different oxygen levels (6 h for anoxia), cells were harvested at 1×10^7 cells/ml for quantitative PCR and Western blot analysis. Multiple ($n \geq 3$) biological replicates were performed for each oxygen treatment. For 0.2% oxygen time-course experiments, *sre1N* cells were transferred into the 0.2% oxygen environment at time 0. Separate cultures were started for each time point such that cells reached a density of 1×10^7 cells/ml at the time of harvest. $n = 4$ biological replicates were performed at each time point. For reoxygenation experiments, *sre1N* cells were first cultured at 0.2% oxygen for 14 h. Separate cultures were removed from the hypoxia workstation and reintroduced to atmospheric oxygen for the indicated duration. Cells were harvested at a density of 1×10^7 cells/ml and frozen for later analysis. $n = 3$ biological replicates were performed at each time point.

Quantitative reverse transcriptase-PCR

S. pombe RNA was harvested as previously described (Hughes *et al.*, 2005). cDNA synthesis was performed as described in the iScript cDNA Synthesis Kit (Bio-Rad, Hercules, CA).

Quantification of Sre1N signal from Western blot analysis

Indicated strains were cultured in rich or minimal media as previously described. Cells were harvested at a density of 1×10^7 cells/ml, and 2×10^7 cells were used for immunoblot analysis. Before SDS–PAGE analysis, samples were treated with alkaline phosphatase to collapse the heavily phosphorylated Sre1N into a single band for quantification (Hughes *et al.*, 2005). Signals from Western blot analysis were quantified as described.

Testing model parameter sets

To find appropriate values for the 11 unknown model parameters (Supplemental Table S2), we constructed parameter sets by picking values for the first seven parameters from appropriate ranges (Supplemental Table S2). For each parameter set, we performed seven computational tests as follows to determine whether the set yielded simulated results consistent with experimental observations. To speed calculations, we ordered the tests such that those involving simple calculations were performed first. Successive tests were only given to parameter sets that had passed all previous tests. When values for the remaining four parameters were required, we determined them by optimization (Supplemental Materials).

1. *Inhibition of Sre1N binding to DNA*: The ability of Ofd1 to keep Sre1N from binding to DNA has been clearly observed in *sre1N-MP ubr1*Δ yeast (Lee *et al.*, 2011). In our model, the *sre1N-MP* mutation, which breaks the ability of Sre1N to up-regulate its own production, is equivalent to setting the parameters $k_{pmXN1} = k_{pmXN2} = 0$ (Hughes and Espenshade, 2008). The *ubr1*Δ mutation, which disables Sre1N degradation, is equivalent to setting the parameters $k_{dXN} = k_{dXNF} = k_{dXNUF} = 0$ (Lee *et al.*, 2011). For each combination of the remaining variable parameters, we required that the model replicate the Ofd1-inhibited DNA binding of Sre1N seen experimentally (Figure 5D in Lee *et al.*, 2011). Specifically, we required the steady-state ratio of free Sre1N under anoxia (0.01% oxygen) to that under normoxia (21% oxygen) to be at least 1.8 to justify the observed increase in DNA binding of Sre1N at low oxygen. At the same time, since deleting *ofd1*$^+$ produces an additional increase in Sre1N binding to DNA, we required the steady-state ratio of free Sre1N to total Sre1N at low oxygen to be no greater than 0.9.
2. *Steady state*: For each set of parameters, we used experimental measurements of *sre1N*$^+$ mRNA at different levels of oxygen (Figure 2A) as inputs to the model and computed the corresponding steady-state levels of Sre1N protein. If R^2 was at least 0.60 for the fit between the logarithms of computed and experimentally measured Sre1N protein (Figure 2B), we computed the amount of free Sre1N protein and then fit a curve between the computed free Sre1N protein ($[X_N]$) and the experimentally measured *sre1N*$^+$ mRNA ($[mX_N]$) to create a positive feedback model:

$$[mX_N] = 1 + \frac{\frac{k_{pmXN1}}{K_{XND1}}[X_N] + \frac{k_{pmXN2}}{K_{XND1}K_{XND2}}[X_N]^2}{1 + \frac{1}{K_{XND1}}[X_N] + \frac{1}{K_{XND1}K_{XND2}}[X_N]^2} \quad (1)$$

   Finding the parameters k_{pmXN1}, k_{pmXN2}, K_{XND1}, and K_{XND2} by optimization (Supplemental Materials) completed the model of oxygen-dependent Sre1N regulation by Ofd1 in *sre1N* cells (Supplemental Eqs. S1–S13 and Figure 1B). With this complete closed-loop model, we computed the steady-state levels of *sre1N*$^+$ mRNA and Sre1N protein at different levels of oxygen and compared the logarithm of the computed values to that of the experimentally measured values (Figure 2, A and B). For the protein comparison, we scaled the computed values such that computed and measured Sre1N protein levels were equal at atmospheric oxygen. We required both comparisons to have $R^2 \geq 0.85$.
3. *Effect of deleting ofd1*$^+$: For each set of parameters, we computed the steady-state ratio of *sre1N*$^+$ mRNA in *sre1N ofd1*Δ yeast to that in *sre1N* yeast. In our experiments, this ratio ranged from 9.7 to 11.3, with an average of 10.3 ($n = 5$; unpublished data). We required $8 \leq$ mRNA ratio ≤ 12. We computed the same ratio for Sre1N protein, which in our experiments ranged from 25.9 to 46.2, with an average of 32.0 ($n = 4$; unpublished data). We required $20 \leq$ protein ratio ≤ 50.
4. *Hypoxia*: For each set of parameters, we performed a time-course simulation in which cells at steady state in atmospheric oxygen were shifted to 0.2% oxygen at $t = 0$ and monitored for 6 h. We compared the simulated trajectories of *sre1N*$^+$ mRNA and Sre1N protein with measurements from the corresponding experiment (Figure 2, D and E). For both of these comparisons, we scaled the computed values such that computed and measured values were equal at $t = 0$. We required both comparisons to have $R^2 \geq 0.85$ calculated from the logarithms of the data. In addition, we required both *sre1N*$^+$ mRNA and Sre1N protein to reach a peak between $t = 1$ and 4 h, consistent with observations.
5. *Recovery from hypoxia*: For each set of parameters, we performed a time-course simulation in which cells at steady state in 0.2% oxygen were shifted to 21% oxygen at $t = 0$ and monitored for 6 h. We compared the half-lives (time to half initial concentration) of *sre1N*$^+$ mRNA and Sre1N protein in simulation with those measured in the corresponding experiment (Figure 2, G and H), requiring $15 \leq t_{1/2} \leq 30$ min for mRNA (22 min experimentally) and $20 \leq t_{1/2} \leq 45$ min for protein (32 min experimentally).
6. *Effect of deleting nro1*$^+$: It has been observed experimentally that *sre1N nro1*Δ cells have lower Sre1N protein levels than untreated *sre1N* cells even when subjected to hypoxia for 3 h (Figure 1F in Lee *et al.*, 2009). For each set of model parameters, we performed a time-course simulation in which *sre1N nro1*Δ cells ($[R_T] = 0$) at steady state in atmospheric oxygen were shifted to 0.01% oxygen for 3 h. We required the level of Sre1N protein at the end of this simulation to be less than that computed in untreated *sre1N* cells at steady state.

7. *Sre1N degradation rate*: In *sre1N* cells grown without oxygen and then shifted to atmospheric oxygen and treated with cycloheximide to inhibit translation, the half-life (time to half initial concentration) of Sre1N protein has been measured to be ~7–9 min (Hughes and Espenshade, 2008; Lee *et al*., 2009). In similarly treated *sre1N ofd1*Δ cells, the half-life of Sre1N has been measured to be ~23 min (Hughes and Espenshade, 2008). To replicate these experiments with the model, for each set of parameters, we performed simulations in which *sre1N* cells at steady state in 0.01% oxygen were shifted to 21% oxygen at $t = 0$ and monitored for 2 h. The effect of cycloheximide was simulated by solving the model equations with parameters $k_{pXN} = k_{pF}^{lowU} = k_{pF}^{highU} = 0$. For *sre1N* cells, we required 4 min ≤ $t_{1/2}$ ≤ 12 min. We repeated these simulations in *sre1N ofd1*Δ cells, solving the model equations with the added initial condition $[F_T] = 0$. For *sre1N ofd1*Δ cells, we required 18 ≤ $t_{1/2}$ ≤ 32 min.

ACKNOWLEDGMENTS

We thank the members of the Iglesias and Espenshade labs for much helpful input during the course of this work. J.R.P. gratefully acknowledges the support of Abel Wolman, Wysocki, and Bowles Fellowships. P.J.E. is an Established Investigator of the American Heart Association. This research was funded by National Institutes of Health Grant HL-077588.

REFERENCES

Bähler J, Wu J-Q, Longtine MS, Shah NG, McKenzie A, Steever AB, Wach A, Philippsen P, Pringle JR (1998). Heterologous modules for efficient and versatile PCR-based gene targeting in *Schizosaccharomyces pombe*. Yeast 14, 943–951.

Barker BM, Kroll K, Vödisch M, Mazurie A, Kniemeyer O, Cramer RA (2012). Transcriptomic and proteomic analyses of the *Aspergillus fumigatus* hypoxia response using an oxygen-controlled fermenter. BMC Genomics 13, 62.

Bien CM, Espenshade PJ (2010). Sterol regulatory element binding proteins in fungi: hypoxic transcription factors linked to pathogenesis. Eukaryot Cell 9, 352–359.

Chang YC, Bien CM, Lee H, Espenshade PJ, Kwon-Chung KJ (2007). Sre1p, a regulator of oxygen sensing and sterol homeostasis, is required for virulence in *Cryptococcus neoformans*. Mol Microbiol 64, 614–629.

Chun CD, Liu OW, Madhani HD (2007). A link between virulence and homeostatic responses to hypoxia during infection by the human fungal pathogen *Cryptococcus neoformans*. PLoS Pathog 3, e22.

Cockman ME, Webb JD, Ratcliffe PJ (2009). FIH-dependent asparaginyl hydroxylation of ankyrin repeat domain-containing proteins. Ann NY Acad Sci 1177, 9–18.

Dayan F, Monticelli M, Pouysségur J, Pécou E (2009). Gene regulation in response to graded hypoxia: the non-redundant roles of the oxygen sensors PHD and FIH in the HIF pathway. J Theor Biol 259, 304–316.

Forsburg SL (1993). Comparison of *Schizosaccharomyces pombe* expression systems. Nucleic Acids Res 21, 2955–2956.

Gordan JD, Simon MC (2007). Hypoxia-inducible factors: central regulators of the tumor phenotype. Curr Opin Genet Dev 17, 71–77.

Henri J, Rispal D, Bayart E, van Tilbeurgh H, Séraphin B, Graille M (2010). Structural and functional insights into *S. cerevisiae* Tpa1, a putative prolyl hydroxylase influencing translation termination and transcription. J Biol Chem 285, 30767–30778.

Hirota K, Semenza GL (2005). Regulation of hypoxia-inducible factor 1 by prolyl and asparaginyl hydroxylases. Biochem Biophys Res Commun 338, 610–616.

Hughes AL, Lee C-YS, Bien CM, Espenshade PJ (2007). 4-Methyl sterols regulate fission yeast SREBP-Scap under low oxygen and cell stress. J Biol Chem 282, 24388–24396.

Hughes AL, Todd BL, Espenshade PJ (2005). SREBP pathway responds to sterols and functions as an oxygen sensor in fission yeast. Cell 120, 831–842.

Hughes BT, Espenshade PJ (2008). Oxygen-regulated degradation of fission yeast SREBP by Ofd1, a prolyl hydroxylase family member. EMBO J 27, 1491–1501.

Hughes BT, Nwosu CC, Espenshade PJ (2009). Degradation of SREBP precursor requires the ERAD components Ubc7 and Hrd1 in fission yeast. J Biol Chem 284, 20512–20521.

Kim HS *et al*. (2010). Crystal structure of Tpa1 from *Saccharomyces cerevisiae*, a component of the messenger ribonucleoprotein complex. Nucleic Acids Res 38, 2099–2110.

Kohn KW, Riss J, Aprelikova O, Weinstein JN, Pommier Y, Barrett JC (2004). Properties of switch-like bioregulatory networks studied by simulation of the hypoxia response control system. Mol Biol Cell 15, 3042–3052.

Lee C-YS, Stewart EV, Hughes BT, Espenshade PJ (2009). Oxygen-dependent binding of Nro1 to the prolyl hydroxylase Ofd1 regulates SREBP degradation in yeast. EMBO J 28, 135–143.

Lee C-YS, Yeh T-L, Hughes BT, Espenshade PJ (2011). Regulation of the Sre1 hypoxic transcription factor by oxygen-dependent control of DNA binding. Mol Cell 44, 225–234.

Osborne TF, Espenshade PJ (2009). Evolutionary conservation and adaptation in the mechanism that regulates SREBP action: what a long, strange tRIP it's been. Genes Dev 23, 2578–2591.

Ozer A, Bruick RK (2007). Non-heme dioxygenases: cellular sensors and regulators jelly rolled into one? Nat Chem Biol 3, 144–153.

Porter JR, Burg JS, Espenshade PJ, Iglesias PA (2010). Ergosterol regulates sterol regulatory element binding protein (SREBP) cleavage in fission yeast. J Biol Chem 285, 41051–41061.

Qutub AA, Popel AS (2006). A computational model of intracellular oxygen sensing by hypoxia-inducible factor HIF1α. J Cell Sci 119, 3467–3480.

Qutub AA, Popel AS (2007). Three autocrine feedback loops determine HIF1α expression in chronic hypoxia. Biochim Biophys Acta Mol Cell Res 1773, 1511–1525.

Saito K, Adachi N, Koyama H, Matsushita M (2010). OGFOD1, a member of the 2-oxoglutarate and iron dependent dioxygenase family, functions in ischemic signaling. FEBS Lett 584, 3340–3347.

Schmierer B, Novak B, Schofield CJ (2010). Hypoxia-dependent sequestration of an oxygen sensor by a widespread structural motif can shape the hypoxic response—a predictive kinetic model. BMC Syst Biol 4, 1139.

Schofield CJ, Ratcliffe PJ (2005). Signalling hypoxia by HIF hydroxylases. Biochem Biophys Res Commun 338, 617–626.

Semenza GL (2010). Oxygen homeostasis. Wiley Interdiscip Rev Syst Biol Med 2, 336–361.

Semenza GL (2011). Oxygen sensing, homeostasis, and disease. N Engl J Med 365, 537–547.

Stewart EV *et al*. (2011). Yeast SREBP cleavage activation requires the Golgi Dsc E3 ligase complex. Mol Cell 42, 160–171.

Todd BL, Stewart EV, Burg JS, Hughes AL, Espenshade PJ (2006). Sterol regulatory element binding protein is a principal regulator of anaerobic gene expression in fission yeast. Mol Cell Biol 26, 2817–2831.

Wehner KA, Schütz S, Sarnow P (2010). OGFOD1, a novel modulator of eukaryotic translation initiation factor 2α phosphorylation and the cellular response to stress. Mol Cell Biol 30, 2006–2016.

Willger SD, Puttikamonkul S, Kim K-H, Burritt JB, Grahl N, Metzler LJ, Barbuch R, Bard M, Lawrence CB, Cramer RA (2008). A sterol-regulatory element binding protein is required for cell polarity, hypoxia adaptation, azole drug resistance, and virulence in *Aspergillus fumigatus*. PLoS Pathog 4, e1000200.